Turkish Journal of Earth Sciences (Turkish J. Earth Sci.), Vol. 20, 2011, pp. 255–271. Copyright ©TÜBİTAK
doi:10.3906/yer-1008-1 First published online 29 November 2010

Geodynamic Significance of the Early Triassic Karaburun Granitoid (Western Turkey) for the Opening History of Neo-Tethys

CÜNEYT AKAL[1], O. ERSİN KORALAY[1], OSMAN CANDAN[1], ROLAND OBERHÄNSLI[2] & FUKUN CHEN[3]

[1] Dokuz Eylül University, Engineering Faculty, Department of Geological Engineering, Tınaztepe Campus, Buca, TR–35160 İzmir, Turkey (E-mail: cuneyt.akal@deu.edu.tr)

[2] Institut für Erd- und Umweltwissenschaften, Universität Potsdam, Karl-Liebknecht Strasse 24, Potsdam 14476, Germany

[3] Chinese Academy of Sciences Key Laboratory of Crust-Mantle Material and Environment, University of Science and Technology of China, Hefei 230026, China

Received 11 August 2010; revised typescript receipt 08 November 2010; accepted 29 November 2010

Abstract: The Karaburun Peninsula, which is considered part of the Anatolide-Tauride Block of Turkey, contains clastic and carbonate sequences deposited on the northern margin of Gondwana. The Palaeozoic clastic sequence, which is intruded by the Early Triassic granitoid and tectonically overlies a Mesozoic mélange sequence, can be divided into three subunits: a lower clastic subunit consisting of a sandstone-shale alternation, an upper clastic subunit consisting of black chert-bearing shales, sandstone and conglomerate, and a Permo–Carboniferous carbonate subunit. The lower Triassic Karaburun I-type granitoid has a high initial $^{87}Sr/^{86}Sr$ ratio (0.709021–0.709168), and low $^{143}Nd/^{144}Nd$ ratio (0.512004–0.512023) and εNd (–5.34 to –5.70) isotopic values. Geochronological data indicate a crystallization (intrusion) age of 247.1±2.0 Ma (Scythian). Geochemically, the acidic magmatism reflects a subduction-related continental-arc basin tectonic setting, which can be linked to the opening of the northern branch of Neo-Tethys as a continental back-arc rifting basin on the northern margin of Gondwana. This can be related to the closure through southward subduction of the Palaeotethys Ocean beneath Gondwana.

Key Words: Karaburun, Neo-Tethys, Palaeo-Tethys, diorite, Triassic, magmatism

Neo-Tetis'in Gelişim Tarihi İçinde Erken Triyas Karaburun Granitoidi'nin (Batı Türkiye) Jeodinamik Önemi

Özet: Türkiye'nin Anatolid-Torid Bloğu'nun bir parçası olarak nitelendirilen Karaburun Yarımadası, Gondvana'nın kuzey kenarında çökelmiş kırıntılı ve karbonatlara ait serileri içermektedir. Erken Triyas yaşlı granitoid tarafından kesilen ve Mezosoyik melanj istifini tektonik olarak üzerleyen Paleozoyik kırıntılı seri üç alt üniteye ayrılabilir: kumtaşı-şeyl ardalanmasından oluşan alt kırıntılı alt-ünite, siyah çört içerikli şeyl ile kumtaşı ve konglomeradan oluşan üst kırıntılı alt-ünitesi ve Permo–Karbonifer karbonat alt-ünite. Erken Triyas yaşlı I-tipi Karaburun granitoidi, yüksek ilksel $^{87}Sr/^{86}Sr$ oranına (0.709021–0.709168), düşük ilksel $^{143}Nd/^{144}Nd$ oranına (0.512004–0.512023) ve εNd (–5.34 ile –5.70) izotopik değerine sahiptir. Jeokronolojik veriler granitoidin kristalizasyon (sokulum) yaşını 247.1±2.0 my (Sikitiyen) olduğunu belirtmektedir. Bu asidik magmatizma dalma-batma ile ilişkili kıtasal-yay tektonik ortam koşullarının yansıtmaktadır. Söz konusu tektonik ortam, Paleo-Tetis Okyanusu'nun güneye doğru, Gondwana altına dalması-batması sırasında Gondwana'nın kuzey kenarı boyunca gelişen kıtasal yay-arkası yırtılma ile ilişkili Neo-Tetis okyanusunun kuzey kolunun açılması şeklinde yorumlanabilir.

Anahtar Sözcükler: Karaburun, Neo-Tetis, Paleo-Tetis, diyorit, Triyas, magmatizma

Introduction

The complex geological structure of Turkey has been shaped by the evolution of the Palaeo- and Neo-Tethyan oceans from Early Palaeozoic to Tertiary time. Throughout the opening and closure histories of these oceans, continental fragments were rifted off from the northern margin of Gondwana, moved northwards and were accreted to Laurasia (Şengör & Yılmaz 1982; Okay *et al*. 1996, 2006; Göncüoğlu & Kozlu 2000; Stampfli 2000; Göncüoğlu *et al*. 2007). Within this long-lived evolution, the İzmir-Ankara-Erzincan suture (Brinkmann 1966), representing closure of the northern branch of Neo-Tethys and continental collision between Laurasia and Gondwana in the Late Cretaceous–Early Tertiary (Figure 1a), is accepted as the main structure in the tectonic classification of the units in Turkey (Ketin 1966; Okay & Tüysüz 1999).

Although a genetic relationship between the closure of Palaeo-Tethys and opening of the Neo-Tethys has been accepted by the great majority of the researchers, the subduction polarity of the Palaeo-Tethys is still controversial. It has been suggested by several workers (Şengör 1979; Şengör & Yılmaz 1981; Okay & Tüysüz 1999; Okay *et al*. 1996; Robertson & Pickett 2000; Göncüoğlu & Kozlu 2000; Göncüoğlu *et al*. 2007) that this ocean was subducting southwards under Gondwana in the Late Palaeozoic–Early Mesozoic, concomitant with the opening of the northern branch of Neo-Tethys as a back-arc rift on the northern margin of Gondwana. However in several papers, the subduction polarity of the Palaeo-Tethys is assumed to be northwards under Laurasia (Okay 2000; Stampfli 2000; Stampfli & Borel 2002; Zanchi *et al*. 2003; Eren *et al*. 2004; Robertson *et al*. 2004; Okay *et al*. 2006).

The Karaburun Peninsula, regarded as part of the Anatolide-Tauride Block, is divided into two main sequences (Figure 1b): a Palaeozoic clastic sequence overlain by Permo–Carboniferous neritic carbonates, and an unconformably overlying Scythian to Maastrichtian carbonate sequence characterized by thick Mesozoic platform-type limestones and dolomites (Figure 1b). This Mesozoic sequence is enclosed in the matrix of the Maastrichtian–Danian Bornova mélange, indicating that Karaburun may occur as a huge allochthonous block in the mélange (Erdoğan *et al*. 1990; Helvacı *et al*. 2009). The existence of granitic intrusions in the Palaeozoic clastic sequence was first described by Türkecan *et al*. (1998). Although a Neogene age was envisaged by Erdoğan (1990), the preliminary Rb/Sr biotite isochron age of 239.0±2.4 Ma (Ercan *et al*. 2000) revealed a possible Triassic age for this intrusion. The present study deals with these granitoid stocks and the surrounding clastic sequence. Results of geochemical and isotopic analyses and U-Pb zircon crystallization age of the granitoid are reported here, and its possible genetic relationship with the closure of the Palaeo-Tethys and related opening of the northern branch of the Neo-Tethys are discussed.

*The geological time scale of Gradstein *et al*. (2004) is used throughout this paper.

Geological Setting and Petrography

The study area, situated in the northern part of the Karaburun Peninsula (Figure 1b), consists of the clastic Karaburun rock association and the tectonically overlying Maastrichtian–Danian Bornova mélange. The clastic sequence is intruded by the Karaburun granitoid (Figure 1c). The clastic sediments, 2 km thick, crop out widely along the western half of the Karaburun Peninsula and can be divided into two subunits. The lower clastic unit (Küçükbahçe Formation; Kozur 1997), which crops out in the western part of the study area, has a monotonous composition and consists mainly of a sandstone-shale alternation. The sandstones are strongly sheared and characteristically have pronounced schistosity. Along the high-strain zones, newly formed fine-grained white mica can be recognized in the field. This unit, which was previously assigned, without any fossil evidence, to the Ordovician (Kozur 1997) or Devonian (Brinkmann *et al*. 1972) is dated as Early Carboniferous age based on newly found microfossils (H. Kozur, pers. com., 2007 in Robertson & Ustaömer 2009). The upper clastic unit is dominated by shales sandstone and fine- to medium-grained conglomerate horizons/lenses are the other lithologies. The existence of *in situ* black chert layers up to 3 m thick and the disappearance of the pronounced schistosity are the most diagnostic features of these clastic rocks. Early Silurian–Late Devonian radiolarians have been extracted from

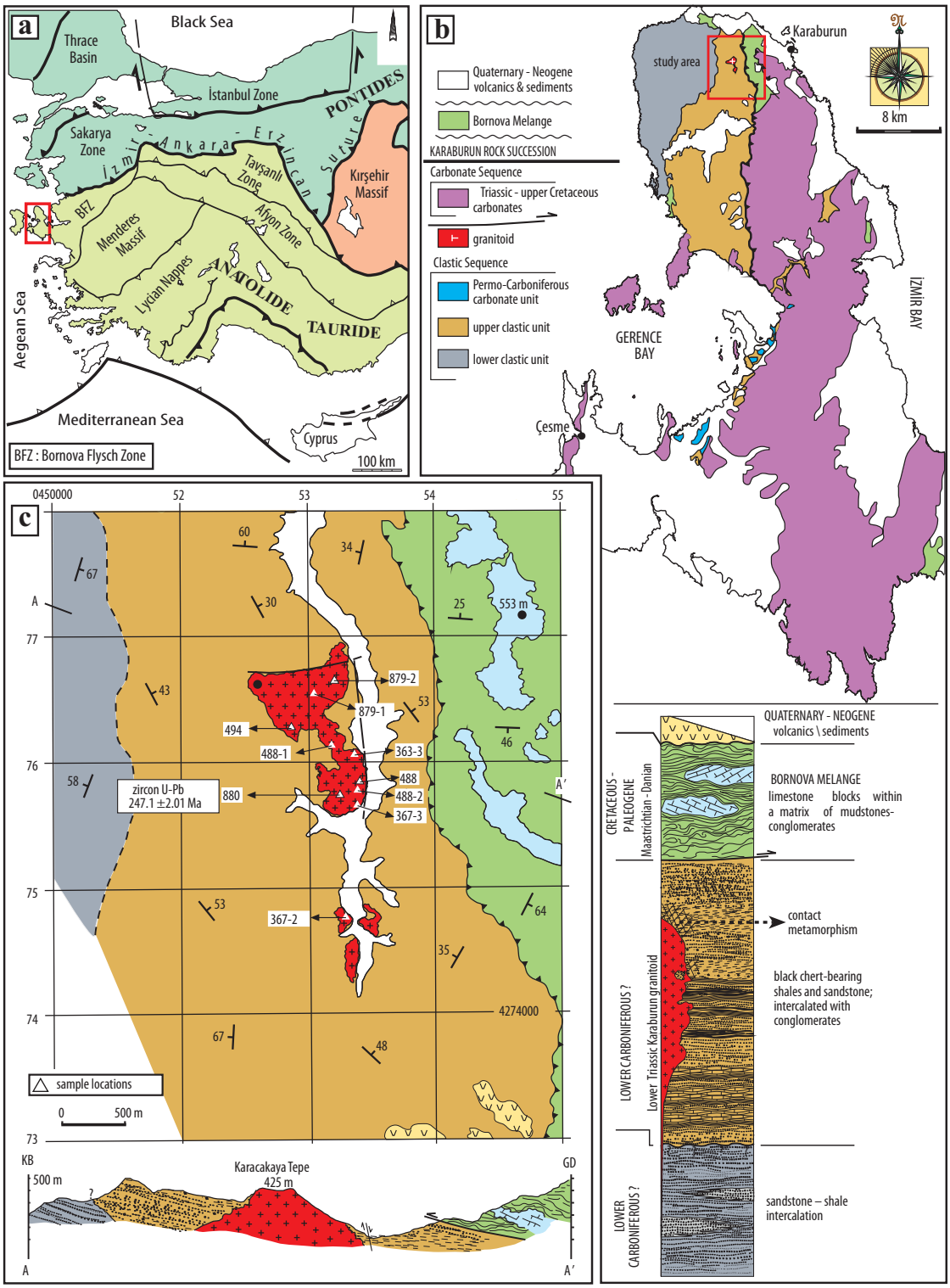

Figure 1. **(a)** Tectonic map of Turkey (simplified after Okay & Tüysüz 1999). **(b)** Geological map of the Karaburun Peninsula and location of the Karaburun granitoid (the map is simplified after Erdoğan 1990 and Çakmakoğlu & Bilgin 2006). **(c)** Geological map, cross-section and columnar section of the study area.

black cherts occurring in the western part of the peninsula (Kozur 1997).

Based on radiometric dating of detrital zircon, an Early Carboniferous age is suggested for this unit (Rosselet & Stampfli 2002). The clastic sequence is tectonically overlain by a mélange consisting of polygenetic blocks, up to 2 km across, embedded in a highly-sheared sandstone-shale matrix. Blocks are dominantly limestones derived from underlying platform-type Mesozoic carbonates. Reddish chert, pelagic carbonate, mafic volcanics and serpentinite constitute the other blocks. Based on the similarities of the internal stratigraphy of the blocks and palaeontological data, this blocky unit was correlated with the Maastrichtian–Danian Bornova mélange by Erdoğan *et al*. (1990).

The granitoid intrusions crop out in the northern part of the Karaburun Peninsula and cover a total area of 1.5 sq km (Figure 1b, c). They occur as two stock-like bodies, measuring 1200 x 600 m and 700 x 400 m, and display intrusive contact relationships with the shales, sandstone and medium-grained conglomerate country rocks. The granitoid stocks consist of diorite to quartz-diorite: aplitic veins are rarely observed in the country rocks. However, close to contact of the stock, xenoliths of the country rock, up to 3 m across, can be observed. The xenoliths are partly assimilated by the granitic melt and have completely recrystallized marginal zones. Especially in the inner parts of large xenoliths the primary sedimentary features are well preserved. The slight contact metamorphism is only developed selectively in the mudstone/shale layers. It is defined by small black spots, up to 1–2 mm across, consisting of white mica and chlorite, most probably pseudomorphous after cordierite.

The Karaburun granitoid is massive and comprises generally fine- to medium-grained (1–5 mm) rocks with an equigranular hypidiomorphic texture (Figure 2a). It shows a compositional variation from diorite to quartz-diorite (Table 1). The mineral assemblage of the granitoid is plagioclase + orthoclase + quartz + biotite + clinopyroxene + hornblende; epidote, apatite, zircon and titanite occur as accessory minerals. Clinopyroxene, the dominant mafic phase in the diorites, forms subhedral grains partly altered to secondary biotite-hornblende assemblages (Figure 2b). The diorite and quartz-diorites are rich in primary hornblende which is closely associated with small biotite crystals. Hornblende occurs as long prismatic crystals. Plagioclases, which are partly altered to white mica, form euhedral to subhedral crystals. Orthoclase is typically found as interstitial crystals among the plagioclase laths. The proportion of the quartz never exceeds 15%.

Analytical Methods

Whole rock, major, trace and rare earth element analyses of 10 fresh samples were conducted by ICP-Emission Spectrometry (Jarrel Ash AtomComp Model 975 / Spectro Ciros Vision) and ICP-Mass Spectrometry (Perkin-Elmer Elan 6000 or 9000) at ACME Analytical Laboratories, Vancouver, British Columbia (Canada). Whole-rock powders were obtained by crushing and splitting from about 15-kg rock samples and milled using the tungsten carbide disc-mill of Retsch RS100 (average milling time is 3 minutes). The selected representative zircons were separated at the Department of Geological Engineering, Dokuz Eylül University. Zircons were isolated from crushed rocks by standard mineral separation techniques and were finally handpicked for analysis under a binocular microscope. Scanning Electron Microscope (SEM) images were obtained with a JEOL JSM-6060 working at 20 kV in the Department of Materials and Metallurgical Engineering; Dokuz Eylül University. Zircon grains studied by cathodoluminescence (CL) were mounted in epoxy resin and polished down to expose the grain centres. CL images were obtained on a microprobe CAMECA SX51 in the Institute of Geology and Geophysics, Chinese Academy of Sciences (IGG CAS).

Isotope measurements of zircons from quartz-diorite sample (880) were performed by laser ablation ICP-MS at the University of Science and Technology of China in Hefei, using an ArF excimer laser system (GeoLas Pro, 193nm wavelength) and a quadrupole ICP-MS (PerkinElmer Elan DRCII). The analyses were carried out with a pulse rate of 10Hz, beam energy of 10J/cm2, and a spot diameter of 60 μm, sometimes 44 μm where necessary. The detailed analytical procedure is similar to Yuan *et al*. (2004). Standard zircon 91500 were analysed to calibrate the

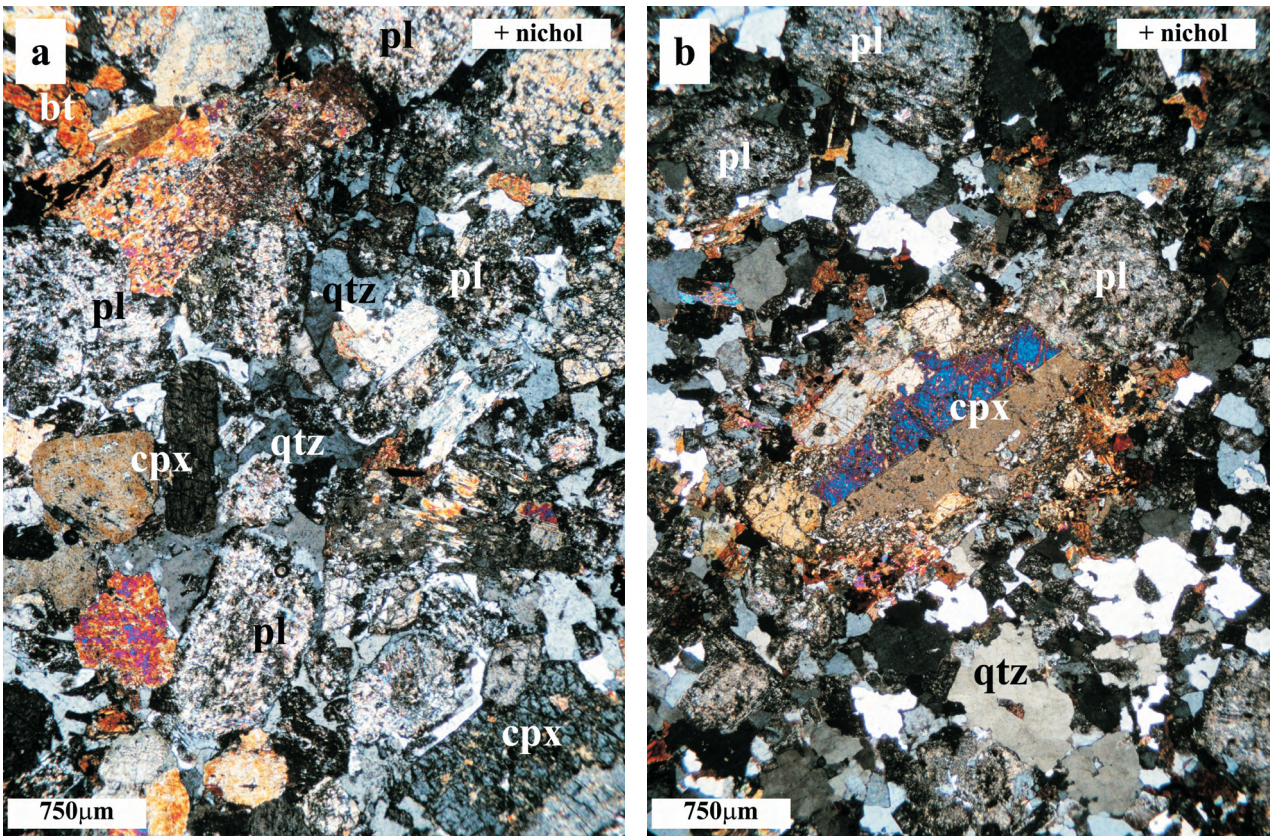

Figure 2. Photomicrographs of the Karaburun granitoid in crossed nicols. **(a)** Typical hypidiomorphic texture of quartz-diorite. Orthoclase (or) and quartz (qtz) occur as interstitial crystals among the plagioclases. **(b)** Clinopyroxene (cpx) phenocrysts which are partly replaced by hornblende (hbl) + biotite (bt) assemblage in quartz-diorite.

mass discrimination and element fractionation; the U/Pb ratios were processed using a macro program LaDating@Zrn written in Excel spreadsheet software. Common Pb was corrected by ComPb corr#3-18 (Anderson 2002). Sm-Nd and Rb-Sr isotopic compositions were measured using a Finnigan MAT-262 mass spectrometer in the LRIG. For Nd-Sr isotope analyses, Rb-Sr and light rare-earth elements were isolated on quartz column by conventional ion exchange chromatography with a 5-ml resin bed of AG 50W-X12 (200-400 mesh). Nd and Sm were separated from other rare-earth elements on quartz columns using 1.7-ml Teflon powder coated with HDEHP, di(2-ethylhexyl) orthophosphoric acid, as a cation exchange medium. Sr was loaded with a Ta-HF activator on pre-conditioned W filaments and was measured in single-filament mode. Nd was loaded as phosphate on pre-conditioned Re filaments and measurements were performed in a Re double filament configuration. The $^{87}Sr/^{86}Sr$ and $^{143}Nd/^{144}Nd$ ratios are normalized to $^{86}Sr/^{88}Sr= 0.1194$ and $^{146}Nd/^{144}Nd= 0.7219$, respectively. In the Laboratory for Radiogenic Isotope Geochemistry of the IGG CAS, repeated measurements of Ames metal and the NBS987 Sr standard in year 2004/2005 gave mean values of 0.512149±0.000003 (n= 98) for the $^{143}Nd/^{144}Nd$ ratio and 0.710244±0.000004 (n= 100) for the $^{87}Sr/^{86}Sr$ ratio. The external precision is a 2σ uncertainty based on replicate measurements on these standard solutions over one year. Total procedural blanks were <300 pg for Sr and <50 pg for Nd.

Geochemistry

Major and trace element compositions of representative Karaburun granitoid samples are given in Table 2. SiO_2 contents of the samples have

Table 1. Major, trace element and isotopic composition of the granitoid located in the north of Karaburun Peninsula, Western Turkey.

Sample No	488	367-3	488-2	363-3	367-2	494	879-1	488-1	880	879-2
Weight percent oxides										
SiO_2	55.77	56.05	56.26	56.33	63.16	65.23	66.53	66.84	67.1	66.52
Al_2O_3	14.51	14.43	14.61	15.33	14.52	14.78	14.35	14.28	14.49	14.00
Fe_2O_3	0.87	0.86	0.86	0.82	0.66	0.51	0.48	0.48	0.43	0.46
FeO	7.92	7.86	7.78	7.41	5.96	4.65	4.17	4.41	3.94	3.94
MgO	6.48	6.44	6.3	5	2.84	2.3	1.97	2.16	1.91	1.91
CaO	7.74	7.78	7.75	7.38	5.07	4.09	3.55	3.03	2.82	2.82
Na_2O	1.6	1.75	1.9	1.89	2	2.48	2.42	2.71	2.55	2.55
K_2O	1.77	1.61	1.59	1.83	2.57	2.95	3.28	2.98	3.33	3.33
TiO_2	0.57	0.54	0.56	0.6	0.73	0.54	0.5	0.49	0.46	0.46
P_2O_5	0.09	0.08	0.09	0.11	0.13	0.11	0.11	0.09	0.11	0.11
MnO	0.15	0.15	0.15	0.14	0.11	0.09	0.09	0.08	0.08	0.08
Cr_2O_3	0.03	0.03	0.03	0.02	0.01	0.01	0.01	0.01	0.01	0.01
LOI	2.3	2.2	1.9	3	2.1	2.1	2.4	2.3	2.7	2.7
Total	99.82	99.81	99.79	99.83	99.87	99.84	99.84	99.84	99.93	99.91
Molar										
K_2O/Na_2O	0.73	0.61	0.55	0.64	0.85	0.78	0.89	0.72	0.86	0.83
K_2O/Al_2O_3	0.13	0.12	0.12	0.13	0.19	0.22	0.25	0.23	0.25	0.28
$(K_2O+Na_2O)/Al_2O_3$	0.31	0.32	0.33	0.33	0.42	0.49	0.52	0.54	0.54	0.61
$Al_2O_3/(CaO+Na_2O+K_2O)$	0.8	0.8	0.8	0.8	0.9	1	1	1.1	1.1	1.1
$Al_2O_3/(Na_2O+K_2O)$	3.2	3.1	3	3	2.4	2	1.9	1.9	1.9	1.6
Mg#	60.7	60.7	60.4	56.0	47.3	48.3	47.1	48.1	47.8	48.1
Parts per million										
Ba	276	247	252	315	377	402	423	403	427	360
Ni	18.4	17.7	16.4	13.3	14.5	9.5	14.6	9.5	9	6.8
Sc	39	38	38	35	25	19	17	18	15	12
Co	49.7	52.2	55.7	58.8	37.2	46.8	50.9	37.3	41.2	34.4
Ga	12.9	12.4	13.8	13.3	14.1	15.1	15.7	13.7	15.3	15.9
Nb	4.2	4	4.9	5.1	8.5	8.2	9.1	8.2	8.6	8.2
Rb	58.1	51.3	56.8	51.6	77.5	105	117.8	99.3	121.7	135.4
Sr	257.7	248.9	256.5	228.9	161.9	181.8	124.9	119.6	150.2	152
Th	3.7	3.8	4.6	6.1	9.1	9.1	11.1	8.4	9.4	8.4
U	1	1.1	1.2	1.6	1.6	2.1	2.7	2.1	2.3	2.4
V	237	224	250	210	159	123	109	103	107	74
Zr	64.6	67.5	74.8	82.2	131.6	135.7	146	138.7	151.5	123.6
Y	13	12.6	14	16.4	18.8	18.2	18	18.4	17.5	15.2
Cu	48.5	46	45.1	31.3	32.4	12.2	15.7	14.7	5.7	3.8
Pb	5.5	5	5.8	8.4	9.3	11.1	17.5	14.1	16.2	13.3
Zn	41	35	29	57	43	45	53	84	48	33
Cs	1.8	1.7	1.8	1.7	1.8	1.9	1.6	1.5	1.6	2.6
Hf	1.8	2	2.1	2.7	3.6	3.9	4.3	4.2	4.6	3.8
W	186.1	216.2	243.9	306.9	209.9	319.7	328.4	249.7	284.8	260.7
Ta	0.3	0.3	0.4	0.4	0.7	0.7	0.8	0.7	0.8	0.8
La	11.6	11.3	12.7	16.3	24.9	20.7	20.9	20	20.1	16.9
Ce	23	22.6	25.4	31.6	49	41.1	40.6	40.1	39	32.6
Pr	3.02	2.86	3.34	3.97	6.16	5.25	5.36	5.27	5.16	4.3
Nd	11.7	11.6	12.7	15.3	22.2	20.1	20	19.6	19.5	15.5
Sm	2.15	2.09	2.45	2.74	3.67	3.65	3.72	3.51	3.53	2.93
Eu	0.63	0.61	0.7	0.71	0.83	0.77	0.81	0.76	0.74	0.67
Gd	2.39	2.37	2.65	3.02	3.66	3.56	3.73	3.67	3.63	2.96
Tb	0.35	0.34	0.37	0.43	0.5	0.49	0.53	0.51	0.51	0.44
Dy	2.43	2.17	2.69	2.95	3.33	3.38	3.48	3.43	3.5	2.89
Ho	0.48	0.48	0.53	0.59	0.68	0.69	0.7	0.69	0.69	0.57
Er	1.42	1.33	1.57	1.79	2.02	1.96	2.00	1.92	1.99	1.67
Tm	0.24	0.21	0.25	0.28	0.31	0.33	0.32	0.33	0.31	0.29
Yb	1.42	1.36	1.53	1.77	1.88	1.92	1.94	1.87	2.02	1.7
Lu	0.22	0.2	0.24	0.26	0.29	0.28	0.29	0.28	0.29	0.25
(La/Yb)CN	5.86	5.96	5.95	6.61	9.5	7.73	7.73	7.67	7.14	7.13
(Ce/Sm)CN	2.67	2.70	2.59	2.88	3.34	2.82	2.73	2.86	2.76	2.78
(Tb/Yb)CN	1.12	1.14	1.10	1.10	1.21	1.16	1.24	1.24	1.15	1.18
Eu/Eu*	0.85	0.84	0.84	0.75	0.69	0.65	0.66	0.65	0.63	0.70
$^{87}Sr/^{86}Sr)_i$	0.709168								0.709021	
$^{143}Nd/^{144}Nd)_i$	0.512023								0.512004	
εNd(t)	-5.34								-5.70	

Mg number = molar 100Mg/(Mg+0.9Fe

Table 2. Laser ablation ICP–MS U-Pb data and calculated ages for zircons from quartz-diorite.

Grain	Isotopic Ratios			Ages		
	$^{207}Pb/^{206}Pb \pm 1\sigma$	$^{207}Pb/^{235}U \pm 1\sigma$	$^{206}Pb/^{238}U \pm 1\sigma$	$^{207}Pb/^{206}Pb \pm 1\sigma$	$^{207}Pb/^{235}U \pm 1\sigma$	$^{206}Pb/^{238}U \pm 1\sigma$
gr 1*	0.05567 ± 0.00619	0.29848 ± 0.03947	0.04052 ± 0.00141	439 ± 233	265 ± 31	256 ± 9
gr 2	0.11236 ± 0.00410	5.52562 ± 0.30536	0.35591 ± 0.01176	1838 ± 54	1905 ± 48	1963 ± 56
gr 3*	0.00521 ± 0.00249	0.27461 ± 0.01768	0.03856 ± 0.00137	290 ± 84	246 ± 14	244 ± 8
gr 4*	0.04605 ± 0.00386	0.24162 ± 0.01912	0.03806 ± 0.00106	± 185	220 ± 16	241 ± 7
gr 5*	0.05264 ± 0.00285	0.29099 ± 0.01961	0.04051 ± 0.00145	314 ± 90	259 ± 15	256 ± 9
gr 6	0.05863 ± 0.00311	0.95096 ± 0.06715	0.11833 ± 0.00411	553 ± 94	679 ± 35	721 ± 24
gr 7*	0.05359 ± 0.00262	0.29555 ± 0.01887	0.04033 ± 0.00140	354 ± 83	263 ± 15	255 ± 9
gr 8	0.08123 ± 0.00309	2.09608 ± 0.11806	0.18674 ± 0.00620	1227 ± 61	1148 ± 39	1104 ± 34
gr 10	0.06481 ± 0.00331	0.49203 ± 0.03277	0.05504 ± 0.00188	768 ± 84	406 ± 22	345 ± 12
gr 11*	0.05036 ± 0.00493	0.26555 ± 0.03357	0.03971 ± 0.00141	211 ± 218	239 ± 27	251 ± 9
gr 12*	0.04929 ± 0.01619	0.24998 ± 0.08157	0.03678 ± 0.00139	162 ± 559	227 ± 66	233 ± 9
gr 13*	0.08071 ± 0.00390	0.91720 ± 0.05948	0.08284 ± 0.00308	1214 ± 71	661 ± 31	513 ± 18
gr 14*	0.05385 ± 0.00260	0.29216 ± 0.01903	0.03953 ± 0.00134	365 ± 87	260 ± 15	250 ± 8

* Analysis used in age calculation.

a wide range of 55.5 and 67.2 wt%. The Mg-numbers (Mg number= molar $Mg/(Mg+0.9Fe_T)$) are rather high, varying within a restricted range of 50–62 wt%. Using the total alkalis versus silica diagram of Cox *et al.* (1979) adapted by Wilson (1989) for plutonic rocks, composition of the Karaburun intrusion ranges from quartz-diorite to diorite (Figure 3). The granitoid can be classified as calc-alkaline in the AFM diagram of Irvine & Baragar (1971) (Figure 4a). The high-K composition of the intrusions can be seen by wt% $K_2O–SiO_2$ diagram which includes the field boundaries of Peccerillo & Taylor (1976) (Figure 4b). Here, the quartz-diorites concentrate in the field of high-K calc-alkaline rocks, whereas diorites plot both on the boundary line separating the high-K and calc-alkaline fields and in the calc-alkaline field.

The degree of alumina saturation of the rocks is shown in Figure 5, a plot of molar A/NK vs the alumina saturation index {ASI= molecular ratio $Al_2O_3/(CaO + Na_2O + K_2O)$}. The rocks with dioritic composition show A/NK molar ratios > 2, while the quartz-diorites have a A/NK molar ratio ranging from 2.4 to 1.6. The granitoid body is transitional between metaluminous and peraluminous. The dioritic rocks are mainly metaluminous with A/CNK < 1 and fall within the field of I-type granites (Chappell & White 1992). The quartz-diorites have a dominant peraluminous composition. They also plot within the I-type granite field or close to separation boundary of Maniar & Piccoli (1989).

In the Rb–(Y+Nb) and $Rb–SiO_2$ discriminatory diagrams of Pearce *et al.* (1984), the Karaburun intrusion falls within the field of granitoids representing active continental margin (continental arc) (Figure 6a). In the tectonic setting discrimination diagram of calc-alkaline magmas of Thieblemont & Tegyey's (1994) the same samples fall into the subduction-related field (Figure 6b). The Th/Yb–Ta/Yb diagram of Pearce (1982, 1983) was revised by Gorton & Schandl (2000) to propose a geochemical index for the definition of three major tectonic zones: oceanic arcs, active continental margins and within-plate volcanics. In this diagram, Karaburun samples are restricted to the active continental margin field (Figure 6c). For magmatic arc granites, the Rb/Y–Y diagram was used as a qualitative indicator of arc maturity (Brown *et al.* 1984). The samples plot within the fields of primitive and normal continental arcs (Figure 7). Therefore, the Karaburun intrusion can be interpreted as having formed in primitive to normal continental magmatic arc environment.

Their REE C1-Chondrite-normalized patterns are highly fractionated and show high LREE/HREE ratios [(La/Yb)N= 5.86–9.50], little LREE fractionation [(Ce/Sm)N= 2.59–3.34] and negative Eu anomalies (Eu/Eu*= 0.63–0.85) (Figure 8). Brown *et al.* (1984) suggested that with increasing maturity, volcanic-arc granitoids are enriched in Rb, Th, U, Ta, Nb, Hf and Y and are depleted in Ba, Sr, P, Zr and Ti. As seen in Figure 9a, in the primordial

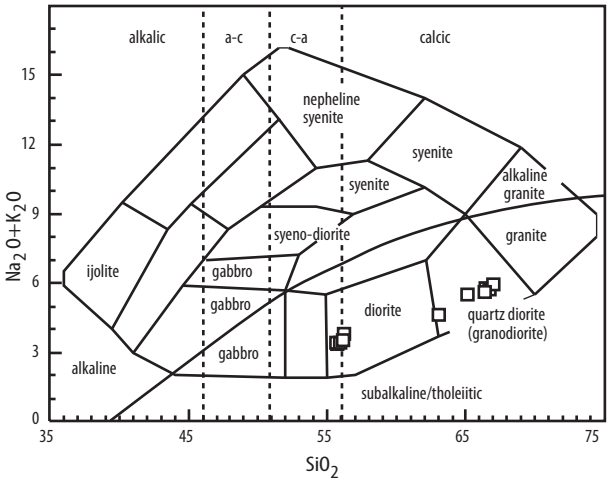

Figure 3. SiO_2–Na_2O+K_2O diagram of Cox *et al.* (1979). The dividing line between the subalkaline and alkaline domains is after Irvine & Baragar (1971).

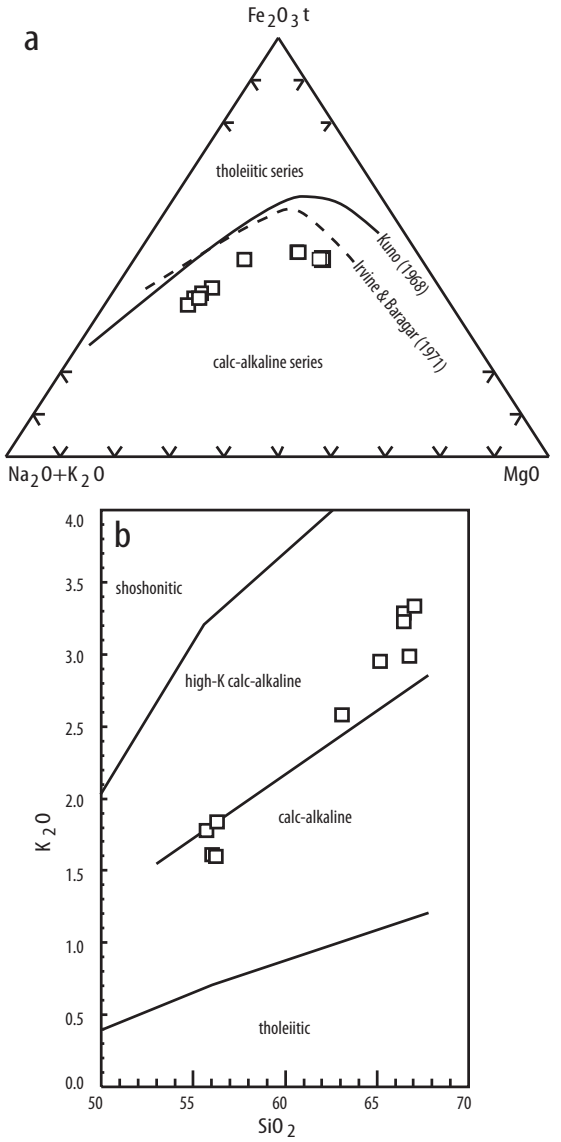

Figure 4. **(a)** AFM diagram illustrating the calc-alkaline trend of the granitoid. **(b)** Major element K_2O–SiO_2 Harker diagram. Field boundaries are after Peccerillo & Taylor (1976).

mantle-normalized (Wood *et al*. 1979) spidergrams, the Karaburun intrusion belongs to the transitional granitic magmatism between primitive and mature continental arc environments described by Brown *et al*. (1984), with some enrichment in highly incompatible elements (e.g., Rb, Ba, K, Nb) and depletion in Sr, P, Zr and Ti. Normalized relative to C1-Chondrite, trace element diagrams of Sun & McDonough (1989), Ba, Rb and Pb contents of the samples are enriched whereas all the samples show superimposed Nb troughs (Figure 9b) and their Sr, P and Ti contents are depleted. Sun & McDonough (1989) suggested that sediment addition and/or an arc signature can cause increases in Rb, Ba, and Pb and decreases in Nb and that Sr is generally enriched in the arc signature and is generally depleted on sediment addition.

U-Pb Geochronology and Isotope Geochemistry

One quartz-diorite sample was chosen for conventional U-Pb age determination. It was taken from the locality where the intrusive contact relationship with upper clastic unit is well exposed (Figure 1c). The zircon concentrations were grouped into different types based on their characteristics of size, colour, morphology, inclusions, turbidity, and abundance of cores and lack of cracks. SEM images show that the zircon grains have heterogeneous morphologies (Figure 10a). They are euhedral, sometimes asymmetric, colourless to slightly pink, transparent, clear to slightly turbid, stubby, short- and long-prismatic with generally 2:1, rarely 3:1 length/width ratios. They occasionally have few inclusions consisting mainly of apatite. According to the classification of Pupin & Turco (1974), these zircons predominantly belong to subtypes S18 and, to a lesser extent, to subtypes S1 and S19. In other words,

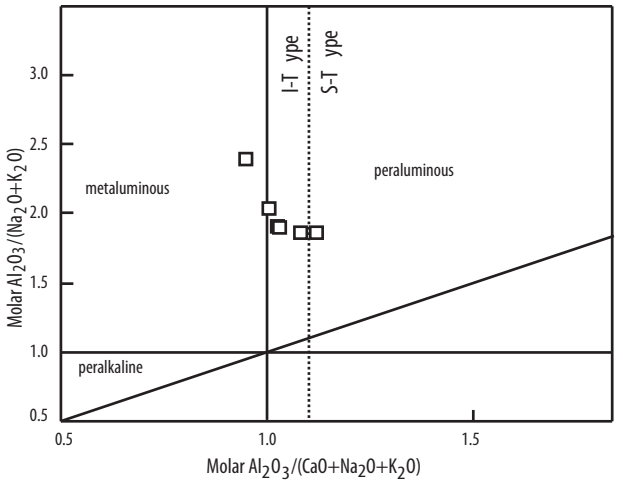

Figure 5. Plots of molar A/NK against ASI {molar Al_2O_3/(CaO +Na_2O+K_2O)} contents of the Karaburun intrusion on the Shand's index diagram. Discrimination line for I-type and S-type granitoid rocks is from Maniar & Piccoli (1989).

the zircons of the quartz-diorite are characterized by a combination of (101)=(211) pyramids and (100)>(110) prisms. CL study revealed the existence of zircons with different textures, magmatic zircons, inherited zircons and zircons with multiple growth stages (Figure 10b). Most of the zircons show typical oscillatory zoning. Some zircon grains have xenocrystic cores preserving oscillatory zoning of magmatic origin.

Fifteen zircons from this sample were subjected to LA-ICP-MS analysis (fifteen point analyses were performed) and thirteen reliable results were obtained. Corrected isotope data and ages are presented in Table 2. Uncertainties in isotope ratios are quoted at the 1σ level and uncertainties in ages are reported at the 95% confidence level. Eight grains of 13 analyzed zircons cluster on the concordia (Figure 11) and define a concordia age of 247.1±2.0 Ma (MSWD of concordance= 0.039), which agrees with the mean $^{207}Pb/^{235}U$ age of 250±12 and mean $^{206}Pb/^{238}U$ age of 247.7±5.8 Ma. The concordia age is interpreted to represent the Scythian intrusion age of the quartz-diorite body. This age is consistent with the previously reported biotite ages of 239.0±2.4 Ma for the same quartz-diorite body (Ercan *et al.* 2000). Three grains display Pb loss and two grains fall on the reverse side of the concordia line. They plot close

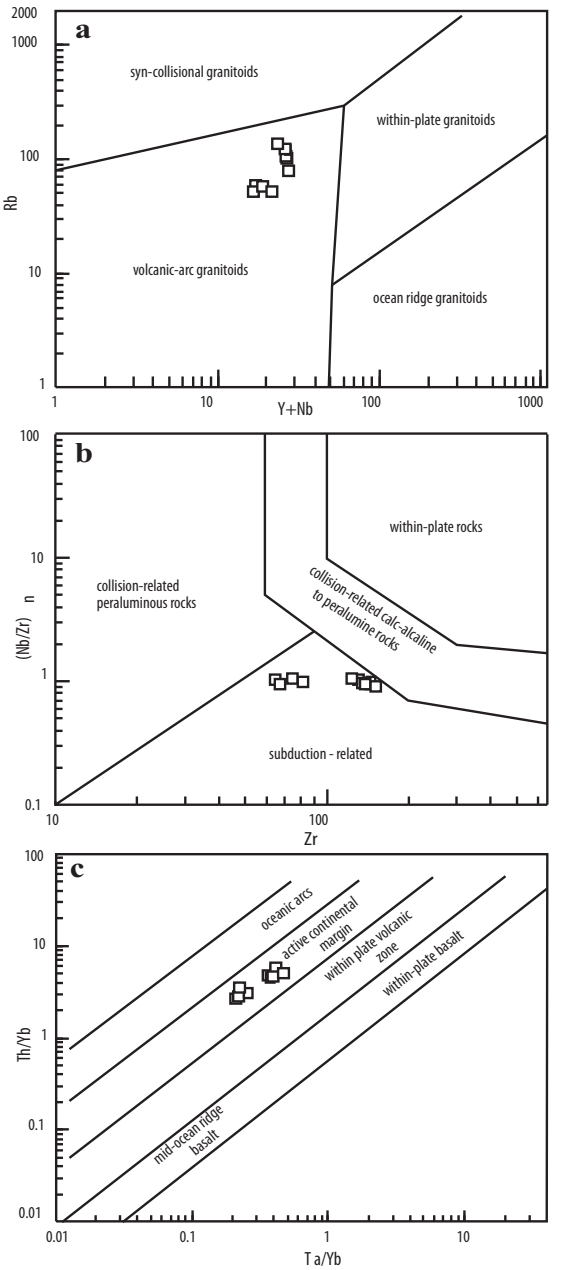

Figure 6. **(a)** Chemical compositions of the Karaburun intrusion in tectonic discrimination diagrams of Pearce *et al.* (1984). **(b)** $(Nb/Zr)_n$–Zr diagram of Thieblemont & Tegyey (1994). Nb and Zr contents of the samples are normalized to Nb and Zr values to the primitive mantle described by Hofmann (1988). **(c)** Th/Y–Ta/Yb geodynamic setting discrimination diagram of Pearce (1982, 1983) revised by Gorton & Schandl (2000) to define tectonic fields.

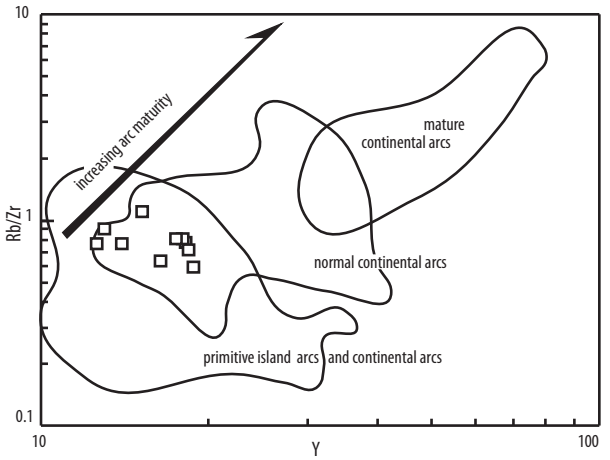

Figure 7. Trace element arc maturity indicators after Brown *et al.* (1984).

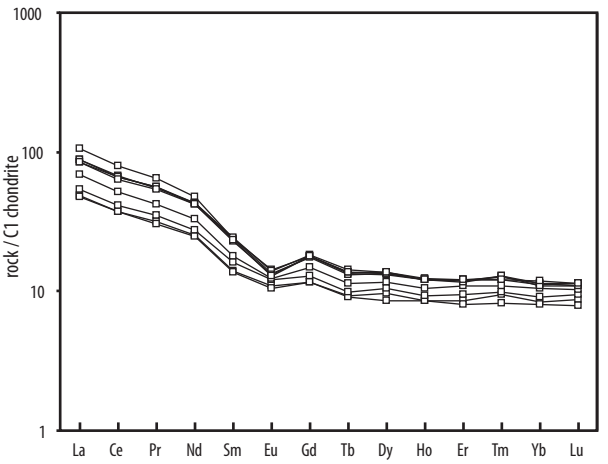

Figure 8. C1-Chondrite-normalized REE patterns of the Karaburun granitoid. Normalized values are after Sun & McDonough (1989).

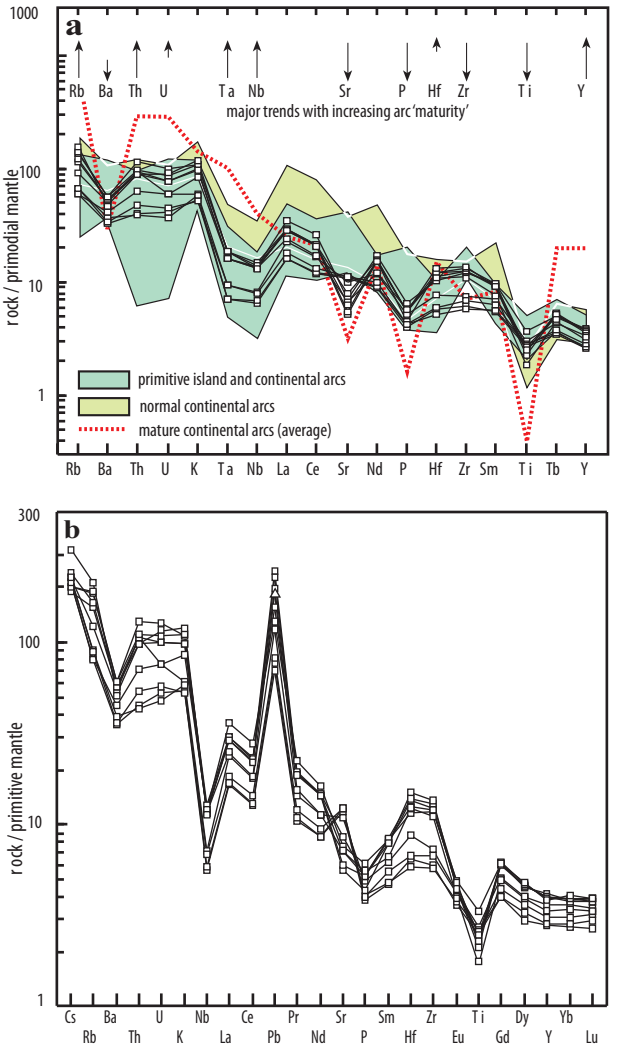

Figure 9. **(a)** Primordial Mantle (Wood *et al.* 1979)-normalized multi-element diagram showing trace element patterns for granitoids from primitive, normal and mature continental arc environments (Brown *et al.* 1984). **(b)** Primitive mantle-normalized abundances of incompatible and compatible trace elements of the Karaburun intrusion. Normalized values are from Sun & McDonough (1989).

to the concordia line and yielded slightly discordant ages. These older ages, between 400 Ma and 1900 Ma, represent the existence of subordinate inherited components.

The whole rock Sr and Nd isotope ratios of representative samples from the granitoid are listed in Table 2 and illustrated in Figure 12. The intrusion has high initial $^{87}Sr/^{86}Sr$ ratios, low $^{143}Nd/^{144}Nd$ ratios and negative εNd. They plot in the enriched quadrant below bulk earth values and approach upper continental crustal values. High $^{87}Sr/^{86}Sr$ ratios and lower $^{143}Nd/^{144}Nd$ ratios of the granitoid rocks are interpreted as recording involvement of lithospheric mantle or continental crust (Hildreth & Moorbath 1988; Rogers & Hawkesworth 1989; Altherr *et al.* 2000).

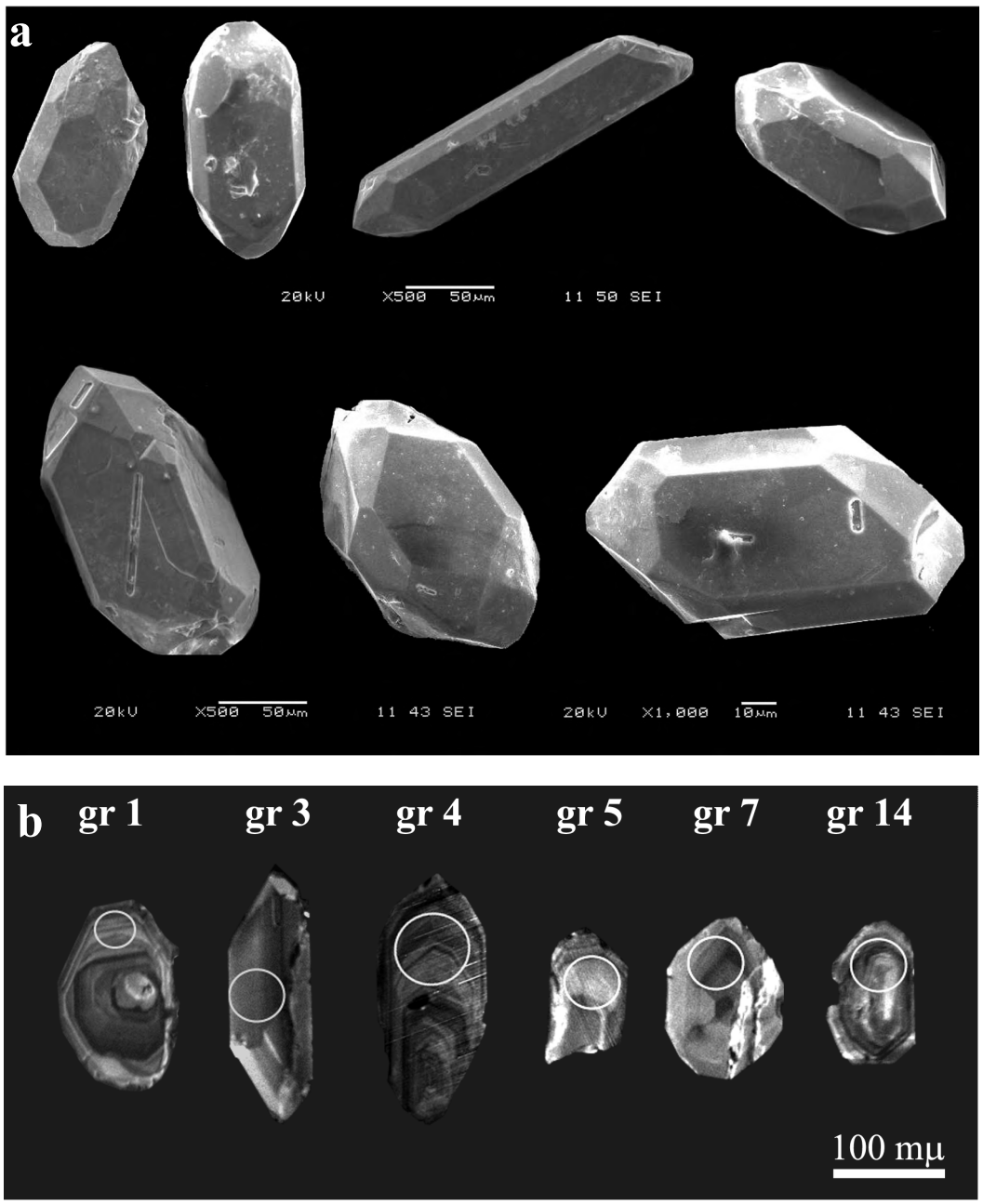

Figure 10. **(a)** SEM images of typical zircons from the Karaburun intrusion. **(b)** Cathodoluminescence (CL) images of selected zircons from quartz-diorite. Spots on zircons represent areas of LA-ICPMS analyses.

Discussion and Conclusion

The Pontides contain geological signatures related to the evolution of Laurasia (Şengör & Yılmaz 1981; Okay & Monie 1997; Topuz *et al.* 2006), whereas the Taurides and their metamorphic equivalents the Anatolides, were deposited on the northern margin of Gondwana and have close relationships with its evolution (Özgül 1983; Okay *et al.* 2001; Göncüoğlu *et al.* 2003; Candan *et al.* 2005). In the general tectonic framework of Turkey, Karaburun is located south of the İzmir-Ankara-Erzincan suture (Figure 1a).

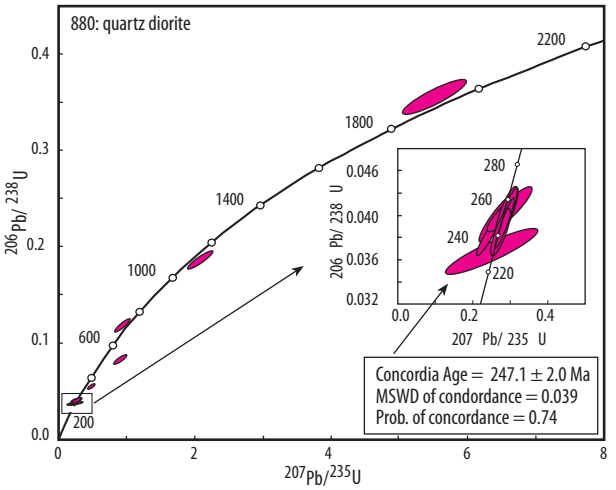

Figure 11. Condordia diagrams showing U-Pb isotope ratios and ages derived from LA-ICPMS analyses for quartz-diorite sample (880).

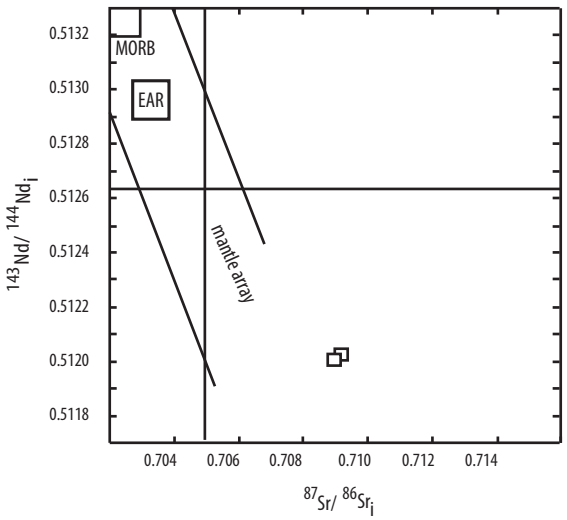

Figure 12. Nd–Sr isotope diagram (initial values) showing data for the Karaburun intrusion. MORB– mid-ocean ridge basalts (Zindler & Hart 1986); EAR– European asthenospheric reservoir (Cebria & Wilson 1995); Mantle Array (De Paolo & Wasserburg 1979).

The most important characteristic of the stratigraphy of the Pontides is the regional Liassic unconformity, separating the basement with Triassic deformation and associated high-pressure metamorphism from a post-Liassic cover series. These are related to the evolution of Laurasia (Okay *et al.* 1996; Okay & Monie 1997). The Lower Triassic–Upper Cretaceous succession of Karaburun is completely free of these events and is characterized by continuous carbonate deposition with local unconformities (Erdoğan *et al.* 1990; İ. Işıntek, unpub. Ph.D. Thesis, Dokuz Eylül University, İzmir 2002; Çakmakoğlu & Bilgin 2006). Based on its Triassic to Upper Cretaceous rock succession, Karaburun is part of the Anatolide-Tauride platform. The Karaburun Palaeozoic basement is dominated by Ordovician(?) to Lower Carboniferous clastic sediments. The Karaburun granitoid intrudes the Lower Carboniferous blocky unit in these clastics. A similar Lower Carboniferous blocky unit has been also reported from Chios island and the Afyon Zone near Konya (Robertson & Pickett 2000; Rosselet & Stampfli 2002; Meinhold *et al.* 2008). The age, deposition environment and tectonic meaning of these blocky units within the general evolution of the Palaeo-Tethys are controversial. Based on the age, internal stratigraphy, rock association and tectonic setting, it was suggested by Robertson & Pickett (2000), Robertson & Ustaömer (2009) and Göncüoğlu *et al.* (2003, 2007) that the Lower Carboniferous blocky unit of the Afyon Zone, which is one of the main tectonic zones of the Anatolides derived from the Anatolide-Tauride platform by Late Cretaceous subduction (Candan *et al.* 2005; Göncüoğlu *et al.* 2007) can be correlated with Karaburun. The continuation of the Karaburun blocky unit to the Afyon Zone and the Triassic to Upper Cretaceous stratigraphy of Karaburun favours a Gondwanan rather than Eurasian affinity for Karaburun between the Carboniferous and Late Cretaceous.

In recent years, many new discoveries have been recorded of widespread magmatism at 246–224 Ma in the Anatolide tectonic zones, especially in the Menderes Massif and Afyon Zone, which correlate with the Karaburun granitoid (Figure 13). Triassic magmatism in the Menderes Massif is characterized by numerous leucocratic granite intrusions in both Pan-African basement and its Palaeozoic cover series (Dannat & Reischmann 1998; Koralay *et al.* 2001). These calc-alkaline intrusions were dated at 235–246 Ma (Early Triassic) using a single zircon evaporation method by Koralay *et al.* (2001). In the Afyon Zone, the common existence of metavolcanic rocks has long been reported (Kurt & Aslaner 1999; Eren *et al.* 2004).

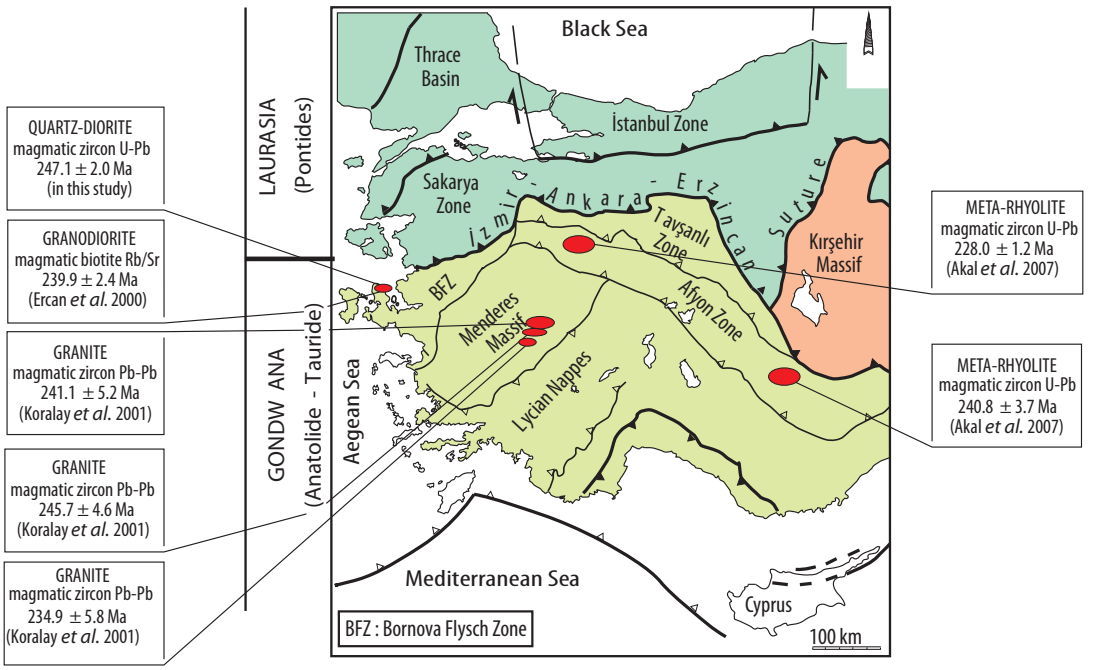

Figure 13. Locations of Triassic magmatism in the Anatolide-Tauride Block.

They form a thick volcanic succession consisting of trachytic, rhyolitic and dacitic lava flows and associated volcaniclastics between the pre-Triassic basement and the Triassic to Upper Cretaceous cover series (Akal *et al.* 2005, 2007). These metavolcanics, which are attributed to the rifting of the northern branch of Neo-Tethys as a consequence of southward subduction of Palaeo-Tethys under the Gondwana margin (Akal *et al.* 2005, 2007; Göncüoğlu *et al.* 2007; Tatar-Erkül *et al.* 2008) were dated at 224–243 Ma by a U/Pb conventional method (Akal *et al.* 2007). Additionally, common undated jadeite and glaucophane-bearing acidic metavolcanics in Triassic metasediments of the Tavşanlı Zone, which was also derived from the northern margin of the Anatolide-Tauride platform, have been documented (Okay & Kelley 1994). Considering the common existence of Early Triassic granites and associated volcanics in the Anatolide tectonic zones, and the Gondwanan affinity of Karaburun during the Permo–Triassic, it can be concluded that the Triassic Karaburun granitoid was intruded within the northern margin of Gondwana. The absence of arc magmatism north of the İzmir-Ankara-Erzincan suture zone is one of the main pieces of geological evidence favouring the south-dipping subduction of Palaeo-Tethys during the Permo–Triassic. The Triassic basic volcanics in the Sakarya Zone are attributed to the uppermost part of an oceanic plateau occurring in Palaeo-Tethys (Okay 2000; Okay *et al.* 2006).

Tectonic models for the tectonic setting of the Karaburun granitoid, as well as the other Early Triassic magmatic rocks in the Anatolides south of the İzmir-Ankara-Erzincan suture, should explain how these magmatic rocks are left on the Gondwana margin by the rifting of the northern branch of Neo-Tethys. This geological restriction can be provided by the flat subduction of the oceanic lithosphere, similar to the Taupo volcanic zone (Collins 2002; Murphy 2006; Collins & Richards 2008), the Eastern Andean Cordillera, Peru (Haeberlin *et al.* 2004) and the western United States (Humphreys *et al.* 2003), under the northern margin of Gondwana during Permo–Triassic time (Figure 14a). In this stage, continental-arc magmatism, which is defined by the intrusion of I-type Karaburun granitoid (247.1±2.0 Ma, Scythian) developed inland of the northern margin of Gondwana (Figure 14a). Slab rollback of oceanic lithosphere commenced crustal extension and caused development of a new back-arc rifting setting. With continuing extension, the northern branch of Neotethys opened and the Karaburun

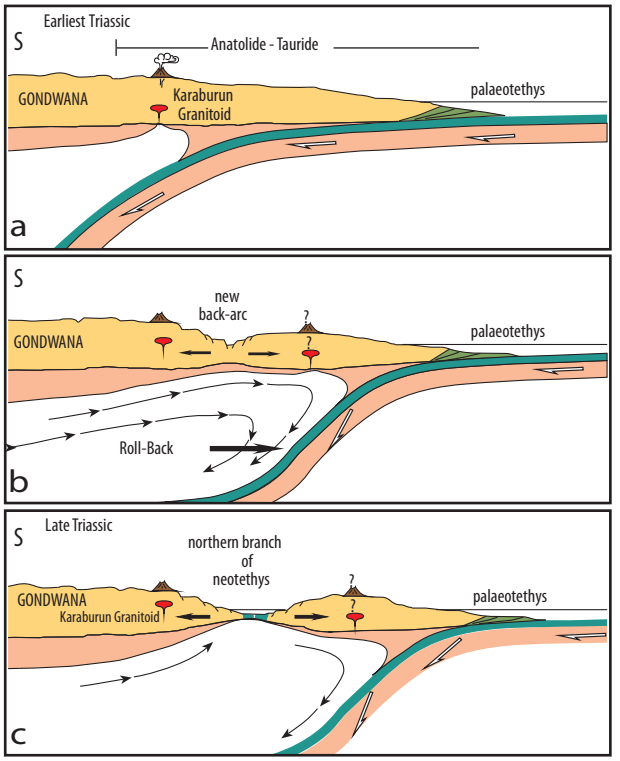

Figure 14. Evolution modelling of Triassic magmatism on the northern margin of Gondwana.

granitoid was left to the south of the back-arc setting on the Gondwana side (Figure 14b). The onset of the oceanic stage of the northern branch of the Neo-Tethys, is marked by a basic volcanic-chert intercalation in Karaburun (Çakmakoğlu & Bilgin 2007) initiated in the Late Triassic (Carnian) (Figure 14c). In our model, new arc magmatism should develop on the continental fragment rifted away from northern margin of Gondwana (Figure 14c). Almost all the tectonic models accept the rifting of a continental fragment (Şengör & Yılmaz 1981) or thin sliver (Okay *et al.* 2006) from Gondwana. But the presence of such a fragment north of the İzmir-Ankara-Erzincan suture is quite controversial (Okay 2000 and references therein). This contradiction can be explained by a model in which the rifted continental fragment, which became attached to the southern margin of Laurasia by the closure of the Palaeo-Tethys was a narrow sliver which became deeply buried by the subduction-continental collision processes during the closure of the northern branch of Neo-Tethys.

Acknowledgements

This project was supported by the Dokuz Eylül University Research Foundation (İzmir, Turkey) (project no. 04.KB.FEN.067) and by Volkswagen-Stiftung, Germany.

References

Akal, C., Candan, O., Koralay, E., Chen, F. & Oberhänsli, R. 2007. *Geochemistry, Geochronology and Tectonic Setting of Early Triassic Metavolcanics of the Afyon Zone, Turkey.* TUBİTAK Project Report, **YDABÇAG-103Y011** [in Turkish with English abstract, unpublished].

Akal, C., Candan, O., Koralay, O.E., Oberhänsli, R. & Chen, F. 2005. Metavolcanic rocks in Afyon Zone: implications for Triassic rifting of Neo-Tethyan Ocean on Gondwanaland. *In: Abstracts, International Symposium on the Geodynamics of Eastern Mediterranean: Active Tectonics of the Aegean. 15–18 June 2005, Kadir Has University, İstanbul,Turkey,* p. 77.

Altherr, R., Holl, A., Hegner, E., Langer, C. & Kreuzer, H. 2000. High-potassium, calc-alkaline I-type plutonism in the European Variscides: northern Vosges (France) and northern Schwarzwald (Germany). *Lithos* **50**, 51–73.

Anderson, T. 2002. Correction of common lead in U-Pb analyses that do not report ^{204}Pb. *Chemical Geology* **29**, 59–79.

Brinkmann, R. 1966. Geotektonische Gliederung von Westanatolien: *Neues Jahrbuch für Geologie und Pal*ä*ontologie-Monatshefte* **10**, 603–618.

Brinkmann, R., Flügel, E., Jacobshagen, V., Lechner, H., Rendel, B. & Trick, P. 1972. Trias, Jura und Kreide der Hlbinsel Karaburun (West-Anatolien). *Geologica et Paleontologica* **5**, 139–150.

Brown, C.G., Thorpe, R.S. & Webb, P.C. 1984. The geochemical characteristics of granitoids in contrasting arcs and comments on magma sources. *Journal of the Geological Society, London* **141**, 411–426.

Çakmakoğlu, A. & Bilgin, Z.R. 2006. Pre-Neogene stratigraphy of the Karaburun Peninsula (W of İzmir Turkey). *Bulletin of the Mineral Research and Exploration Institute (MTA) of Turkey* **132**, 33–62.

Candan, O., Çetinkaplan, M., Oberhänsli, R., Rimmele, G. & Akal, C. 2005. Alpine high-P/low-T metamorphism of the Afyon Zone and implications for the metamorphic evolution of Western Anatolia, Turkey. *Lithos* **84**, 102–124.

Cebria, J.M. & Wilson, M. 1995. Cenozoic mafic magmatism in Western/Central Europe: a common European asthenospheric reservoir? *Terra Abstracts* **8**, p. 162.

Chappell, B.W. & White, A.J.R. 1992. I- and S-type granites in the Lachlan fold belt. *Transactions of the Royal Society of Edinburgh-Earth Sciences* **83**, 1–26.

Collins, W.J. 2002. Hot orogens, tectonic switching and creation of continental crust. *Geology* **31**, 535–538.

Collins, W.J. & Richards, S.W. 2008. Geodynamic significance of S-type granite in circum-Pacific orogens. *Geology* **36**, 559–562.

Cox, K.G., Bell, J.D. & Pankhurst, R.J. 1979. *The Interpretation of Igneous Rocks*. George, Allen and Unwin, London.

Dannat, C. & Reischmann, T. 1998. Geochronological, geochemical and isotopic data on granitic gneisses from the Menderes Massif, SW Turkey. *3rd International Turkish Geology Symposium, Ankara, Abstracts,* p. 282.

De Paolo, D.J. & Wasserburg, G.J. 1979. Petrogenetic mixing models and Nd–Sr isotopic patterns. *Geochimica et Cosmochimica Acta* **43**, 615–627.

Ercan, T., Türkecan, A. & Satır, M. 2000. Karaburun Yaramadasının Neojen volkanizması [Neogene volcanism of Karaburun Peninsula]. *In: Proceedings, Cumhuriyetin 75. Yıldönümü Yerbilimleri ve Madencilik Kongresi.* Mineral Research and Exploration Institute (MTA) of Turkey, Ankara, 1–18.

Erdoğan, B. 1990. Tectonic relations between İzmir-Ankara Zone and Karaburun Belt. *Bulletin of the Mineral Research and Exploration Institute (MTA) of Turkey* **110**, 1–15.

Erdoğan, B., Altiner, D., Güngör, T. & Özer, S. 1990. Stratigraphy of Karaburun Peninsula. *Bulletin of the Mineral Research and Exploration Institute (MTA) of Turkey* **111**, 1–23.

Eren, Y., Kurt, H., Rosselet, F. & Stampfli, G.M. 2004. Palaeozoic deformation and magmatism in the northern area of the Anatolide Block (Konya), witness of the Paleo-Tethys active margin. *Eclogae Geologicae Helvetiae* **97**, 293–306.

Göncüoğlu, M.C., Çapkinoğlu, S., Gürsü, S., Noble, P., Turhan, N., Tekin, U.K., Okuyucu, C. & Göncüoğlu, Y. 2007. The Mississippian in the Central and Eastern Taurides (Turkey): constraints on the tectonic setting of the Tauride-Anatolide Platform. *Geologica Carpathica* **58**, 427–442.

Göncüoğlu, M.C. & Kozlu, H. 2000. Early Paleozoic evolution of the NW Gondwanaland: data from southern Turkey and surrounding regions. *Gondwana Research* **3**, 315–324.

Göncüoğlu, M.C., Turhan, N. & Tekin, K. 2003. Evidence for the Triassic rifting and opening of the Neotethyan İzmir-Ankara Ocean, northern edge of the Tauride-Anatolide Platform, Turkey. *Bulletin of Geological Society Italy Special Volume* **2**, 203–212.

Gorton, M.P. & Schandl, E.S. 2000. From continents to island arcs: a geochemical index of tectonic setting for arc-related and within plate felsic to intermediate volcanic rocks. *Canadian Mineralogist* **38**, 1065–1073.

Gradstein, F.M., Ogg, J.G., Smith, A.G., Bleeker, W. & Lourens, L.J. 2004. A new geological time scale, with special reference to Precambrian and Neogene. *Episodes* **27**, 83–100.

Haeberlin, Y., Moritz, R. & Fontboté, L. 2004. Carboniferous orogenic gold deposits at Pataz, Eastern Andean Cordillera, Peru: geological and structural framework, paragenesis, alteration, and $^{40}Ar/^{39}Ar$ geochronology. *Economic Geology* **99**, 73–112.

Helvaci, C., Ersoy, Y., Sözbilir, H., Erkül, F., Sümer, Ö. & Uzel, B. 2009. Geochemistry and $^{40}Ar/^{39}Ar$ geochronology of Miocene volcanic rocks from the Karaburun Peninsula: implications for amphibole-bearing lithospheric mantle source, Western Anatolia. *Journal of Volcanology and Geothermal Research* **185**, 181–202.

Hildreth, W. & Moorbath, S. 1988. Crustal contributions to arc magmatism in the Andes of Central Chile. *Contributions to Mineralogy and Petrology* **98**, 455–489.

Hofmann, A.W. 1988**.** Chemical differentiation of the earth: the relationship between mantle, continental crust, and oceanic crust. *Earth and Planetary Science Letters* **90**, 297–314.

Humphreys, E., Hessler, E., Dueker, K., Farmer, C., Erslev E. & Atwater, T. 2003. How Laramide-age hydration of North American lithosphere by the Farallon slab controlled subsequent activity in the western United States. *International Geology Review* **45**, 575–595.

Irvine, T.N. & Baragar, W.R.A. 1971. A guide to the chemical classification of the common volcanic rocks. *Canadian Journal of Earth Sciences* **8**, 523–448.

Ketin, İ. 1966. Tectonic units of Anatolia (Asia Minor). *Bulletin of the Mineral Research and Exploration Institute (MTA) of Turkey* **66**, 20–34 [in Turkish with English abstract].

Koralay, O.E., Satir, M. & Dora, O. Ö. 2001. Geochemical and geochronological evidence for Early Triassic calc-alkaline magmatism in the Menderes Massif, western Turkey. *International Journal of Earth Sciences* **89**, 822–835.

Kozur, H. 1997. The age of the siliciclastic series (Karareis Formation) of the Western Karaburun Peninsula, Western Turkey. *In*: Szaniawski, H. (ed), *Proceedings of Sixth European Conodont Symposium (ECOS VI). Palaeontologia Polonica* **58**, 171–189.

Kurt, H. & Arslan, M. l999. Kadınhanı (Konya) K'ca zengin metatrakiandezitinin jeokimyası ve petrojenezi: Devoniyen(?) volkanizmasının gelişimi [Geochemistry and petrogenesis of Kadınhanı (Konya) K-rich metatrachyandesite: the evolution of Devonian (?) volcanism]. *Geological Bulletin of Turkey* **42**, 57–69 [in Turkish with English abstract].

Maniar, P.D. & Piccoli, P.M. 1989. Tectonic discrimination of granitoids. *Geological Society of America Bulletin* **101**, 635–643.

Meinhold, G., Reischmann, T., Kostopoulos, D., Lehnert, O., Matukov, D. & Sergeev, S. 2008. Provenance of sediments during subduction of Paleo-Tethys: detrital zircon ages and olistolith analysis in Palaeozoic sediments from Chios Island, Greece. *Palaeogeography Palaeoclimatology Palaeoecology* **263**, 71–91.

Murphy, J.B. 2006. Arc magmatism I: relationship between tectonic evolution and petrogenesis. *Geoscience Canada* **33**, 145–167.

Okay, A.I. 2000. Was the Late Triassic orogeny in Turkey caused by the collision of an oceanic plateau? *In:* Bozkurt, E., Winchester, J.A. & Piper, J.A.D. (eds), *Tectonics and Magmatism in Turkey and the Surrounding Area.* Geological Society, London, Special Publications **173**, 25–41.

Okay, A.I. & Kelley, S.P. 1994. Tectonic setting, petrology and geochronology of jadeite + glaucophane and chloritoid + glaucophane schists from northwest Turkey. *Journal of Metamorphic Geology* **12**, 455–466.

Okay, A.I. & Monie, P. 1997. Early Mesozoic subduction in the eastern Mediteranean : evidence from Triassic eclogites from northwest Turkey. *Geology* **25**, 595–598.

Okay, A.I., Satir, M., Maluski, H., Siyako, M., Monie, P., Metzger, R. & Akyüz, S. 1996. Palaeo- and Neo-Tethyan events in northwestern Turkey: geologic and geochronologic constraints. *In*: Yin, A. & Harrison, M. (eds), *Tectonic of Asia*. Cambridge University Press, 420–441.

Okay, A.I., Satir, M. & Siebel, W. 2006. Pre-Alpide orogenic events in the Eastern Mediterranean region. *In: European Lithosphere Dynamics.* Geological Society, London, Memoirs **32**, 389–405.

Okay, A.I., Tansel, İ. & Tüysüz, O. 2001. Obduction, subduction and collusion as reflected in the Upper Cretaceous–Lover Eocene sedimentary record of western Turkey. *Geological Magazine* **138**, 117–142.

Okay, A.I. & Tüysüz, O. 1999. Tethyan sutures of northern Turkey. *In*: Durand, B. Jolivet, L., Horváth, F. & Séranne, M. (eds), *The Mediterranean Basin: Tertiary Extension within the Alpine Orogen.* Geological Society, London, Special Publications **156**, 475–515.

Özgül, N. 1983. Stratigraphy and tectonic evolution of the Central Taurides. *In*: Tekeli, O. & Göncüoğlu, M.C. (eds), *Geology of the Taurus Belt, Proceedings of the International Tauride Symposium*. Mineral Research and Exploration Institute (MTA) of Turkey, 77–90.

Pearce, J.A. 1982. Trace element characteristics of lavas from destructive plate boundaries. *In*: Thorpe, R. S. (ed), *Andesites; Orogenic Andesites and Related Rock*. John Wiley and Sons, 525–548.

Pearce, J.A. 1983. Role of sub-continental lithosphere in magma series at active continental margins. *In*: Hawkesworth, C.J. & Norry, M.J. (eds) *Continental Basalts and Mantle Zenoliths.* Shiva Chesire, UK, 230–249.

Pearce, J.A., Harris, N.B.W. & Tindle, A.G. 1984. Trace element discrimination diagrams for the tectonic interpretation of granitic rocks. *Journal of Petrology* **25**, 956–983.

Peccerillo, A. & Taylor, J.R. 1976. Geochemistry of upper Cretaceous volcanic rocks from the Pontic chain, northern Turkey. *Bulletin Volcanologuque* **39**, 557–569.

Pupin, J.P. & Turco, G. 1974. Application a quelques roches endogenes du massif franco-italien de l'Argentera-Mercantour, une typologie originale du zircon accessorie Etude comparative avec la methode des RMA. *Bulletin de la Société Francaise de Mineralogie et de Cristallographie* **97**, 59–69.

Robertson, A.H.F. & Pickett, E.A. 2000. Palaeozoic–Early Tertiary Tethyan evolution of mélanges, rift and passive margin units in the Karaburun Peninsula (western Turkey) and Chios Island (Greece). *In*: Bozkurt, E., Winchester, J.A. & Piper, J.D.A. (eds), *Tectonic and Magmatism in Turkey and the Surrounding Area.* Geological Society, London, Special Publications **173**, 43–82.

Robertson, A.H.T. & Ustaömer, T. 2009. Formation of the Late Palaeozoic Konya Complex and comparable units in southern Turkey by subduction-accretion processes: implications for the tectonic development of Tethys in the Eastern Mediterranean region. *Tectonophysics* **473**, 113–148.

Robertson, A.H.F., Ustaömer, T., Pickett, E., Collins, A., Andrew, T. & Dixon, J.E. 2004. Testing models of Late Palaeozoic–Early Mesozoic orogeny in Western Turkey: support for an evolving open-Tethys model. *Journal of the Geological Society, London* **161**, 501–511.

Rogers, G. & Hawkesworth, C.J. 1989. A geochemical traverse across the North Chilean Andes: evidence for crust generation from the mantle wedge. *Earth and Planetary Science Letters* **91**, 271–285.

Rosselet, F. & Stampfli, G. 2002. The Paleotethys siliciclastic sequence in Karaburun. *EGS/AGU-EUG Joint Assembly, Abstract,* EAE03-A-09770.

Şengör, A.M.C. 1979. Mid-mesozoic closure of Permo–Triassic Tethys and its implications. *Nature* **279**, 590–593.

Şengör, A.M.C. & Yilmaz, Y. 1981. Tethyan evolution of Turkey: a tectonic approach. *Tectonophysics* **75**, 181–241.

Stampfli, G.M. 2000. Tethyan oceans. *In*: Bozkurt, E., Winchester, J.A. & Piper, J.D.A. (eds), *Tectonic and Magmatism in Turkey and the Surrounding Area*. Geological Society, London, Special Publications **173**, 1–23.

Stampfli, G.M. & Borel, G.D. 2002. A plate tectonic model for the Palaeozoic and Mesozoic constrained by dynamic plate boundaries and restored synthetic oceanic isochrones. *Earth and Planetary Science Letters* **169**, 17–33.

Sun, S.-S. & Mcdonough, W.F. 1989. Chemical and isotopic systematics of oceanic basalts; implications for mantle composition and processes. *In*: Saunders, A.D. & Norry, M.J. (eds), *Magmatism in the Ocean Basins Saunders*. Geological Society, London, Special Publications **42**, 313–345.

Tatar-Erkül, S., Sözbilir, H., Erkül, F., Helvaci, C., Ersoy, Y. & Sümer, Ö. 2008. Geochemistry of I-type granitoids in the Karaburun Peninsula, West Turkey: evidence for Triassic continental arc magmatism following closure of the Palaeotethys. *Island Arc* **17**, 394–418.

Thieblemont, D. & Tegyey, Y. 1994. Geochemical discrimination of differentiated magmatic rocks attesting for the variable origin and tectonic setting of calc-alkaline magmas. *Comptes Rendus de l'Academie des Sciences Series IIA, Earth and Planetary Science* **319**, 87–94.

Topuz, G., Altherr, R., Schwarz, W.H., Dokuz, A. & Meyer, H.P. 2006. Variscan amphibolite-facies rocks from the Kurtoğlu metamorphic complex (Gümüşhane area, Eastern Pontides, Turkey). *International Journal of Earth Sciences* **96**, 861–873.

Türkecan, A., Ercan, T. & Sevin, D. 1998. *Neogene Volcanism of the Karaburun Peninsula*. General Directorate of the Mining Research and Exploration (MTA) of Turkey Report no. **10185**, Turkey.

Wilson, M. 1989. *Igneous Petrogenesis.* Unwin Hyman Press, London.

Wood, D.A., Tarney, J., Varet, J., Saunders, A.D., Bougault, H., Joron, J.L., Treuil, M. & Cann, J.R. 1979. Geochemistry of basalts drilled in the North Atlantic by IPOD LEG 49: implications for mantle heterogeneity. *Earth and Planetary Science Letters* **42**, 77–97.

Yuan, H.L., Gao, S., Liu, X. M., Li, H., Günther, D. & Wu, F. 2004. Accurate U-Pb age and trace element determinations of zircon by laser ablation-inductively coupled plasma-mass spectrometry. *Geostandards and Geoanalytical Research* **28**, 353–370.

Zanchi, A., Garzanti, E., Larghi, C. & Gaetani, M. 2003. The Variscan orogeny in Chios (Greece): Carboniferous accretion along a Palaeotethyan active margin. *Terra Nova* **15**, 213–223.

Zindler, A. & Hart, S. 1986. Chemical geodynamics. *Annual Review of Earth and Planetary Sciences* **14**, 493–571.

Scientific Editing by Ercan Aldanmaz